Simulative analysis for static and dynamic behaviour of QT800-2 ductile iron crankshaft

ZEMIN FU*, GUANGMING LIU
School of Mechanical Engineering, Shanghai Institute of Technology, Shanghai, P.R. China

A three–dimensional finite element model of S195 diesel engine's crankshaft, established with ABAQUS analysis platform, is proposed in this paper for investigating the actual working conditions of crankshaft running. The finite element simulation was used to analyses the vibration modal and the distortion and stress status of the crankthrow. The maximum deformation, maximum stress point and dangerous areas are found by the stress analysis of crankthrow. The relationship between the frequency and the vibration modal is explained by the modal analysis of crankshaft. The results would provide a valuable theoretical foundation for the optimization and improvement of engine design.

(Received August 5, 2013; accepted January 22, 2014)

Keywords: Crankshaft, Finite element analysis, Fatigue strength, Modal analysis, Stress analysis

1. Introduction

Crankshaft is one of the most important moving parts in internal combustion engine [1]. It must be strong enough to take the downward force of the power stroked without excessive bending, to bear gas pressure of cylinder, cyclically changed load caused by reciprocating and rotating mass inertial force. So the reliability and life of internal combustion engine depend on the strength of the crankshaft largely. And as the engine runs, the power impulses hit the crankshaft in one place and then another. The torsional vibration appears when a power impulse hits a crankpin toward the front of the engine and the power stroke ends. It may also undertake bending and axial vibration. If not controlled, all of these may lead to fatigue failure of crankshaft, bringing about downtime, machine damage and even body injury. Consequently it is of great significance for guiding crankshaft optimization and improving engine design how to get more accurate stress, size and distribution of deformation and natural frequency and vibration shape of crankshaft.

Though there are literatures on the three-dimensional finite element modeling method of diesel crankshaft with ANSYS platform [2-6], there exists no small simulation error. Therefore, this study attempts to establish a crankshaft model with ABAQUS static and steady as well as dynamic and non-linear analysis platform, and check its applicability from the view point of making the production process more efficient.

In the paper, 3-D finite element analyses are carried out on the modal analysis of crankshaft and the stress analysis of crankpin. And the FME software ABAQUS was used to simulate the modal analysis and crankshaft. The results of natural frequencies and mode shape were obtained. And stress and deformation distributions of crankpin were obtained by using ABAQUS software. The results are regarded as a theory basis to optimize the design of crankshaft and analysis the structure dynamics of crankshaft.

2 Finite element simulation of crankshaft

2.1 simulation algorithm

The crankshaft running is an extremely complicated physical process. It is a high non-linear problem including geometric non-linear, material non-linear and contact non-linear. To solve this, the explicit algorithm of ABAQUS/Explicit module fitted for dynamic and non-linear analysis could be used to simulate the dynamic behavior of crankshaft, and the implicit algorithm of ABAQUS/standard module adapted to static and steady analysis to simulate the static behavior of crankshaft [7].

2.2 Simulation setup

2.2.1 Material parameters

The main dimensions of crankshaft of S195 engine selected in the analysis include that the diameter of link neck is 65mm, the diameter of spindle is 70mm, the length of crank is 308mm. The crankshaft is made from QT800-2, whose material property is shown in Table 1.

Table 1. Material properties.

Item	Value
Material	QT800-2
Y (yield strength)/MPa	480
E (elastic modulus)/MPa	174000
Density/($g \cdot cm^{-2}$)	7.30
Poisson ratio	0.27

2.2.2 Finite element mesh

Taking the geometry of the crankshaft into account, the paper uses the three-dimensional solid elements in the finite element modeling [8]. According to mechanical analysis, the force at the link neck and the spindle is bigger than the other parts and mesh more intensively; the stress concentrate in the fillet which is the crankshaft dangerous point and the mesh is densest while the mesh in the crank arm is sparse. The model is shown in Fig. 1, the total number of nodes is 36299, and elements are 139,086. Use the continuum solid element C3D8 in finite element model during analysis of the crankshaft [9].

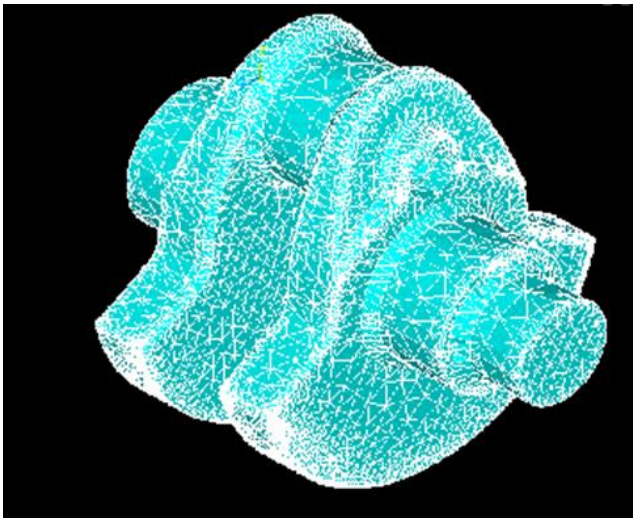

Fig. 1. Mesh of crankshaft.

2.2.3 Load handling

In the course of the crankshaft's work, the reciprocating inertia force P_j and the combustion gas pressure P_g are passed to the crankshaft through the piston and link rods. Taking the uneven quality centrifugal force Pr into account, shear force T and the neck force Z acting on the crankshaft generate. Deduce from Fig. 2

$$\sum P = P_g + P_J \quad (1)$$

$$T = \sum P \times \frac{\sin(\alpha + \beta)}{\cos \beta} \quad (2)$$

$$Z = \sum P \times \frac{\cos(\alpha + \beta)}{\cos \beta} - P_r \quad (3)$$

$$P_g = (p_g - p') \times \frac{\pi}{4} D^2 \quad (4)$$

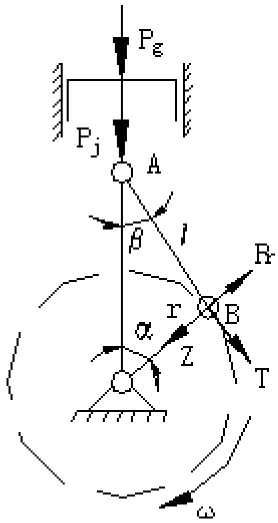

Fig. 2. The load force of crankshaft.

Where P_g is the gas force, P_j is the reciprocating inertia force, P_r is the unbalance centrifugal force; α is the crank rotation angle, β is the swing angle for the connecting rod; D is the cylinder diameter, p_g is the absolute pressure inside the cylinder, p' is the absolute gas pressure of the crankcase, and generally $p' = 10^5$ Pa for the four-stroke diesel engines.

Acceleration of piston can be obtained from kinematics knowledge of the crank and linkage mechanism.

$$a = r\omega^2\{\cos\alpha + \lambda[(1-\lambda^2\sin^2\alpha)\cos 2\alpha + \frac{\lambda^2}{4}\sin^2 2\alpha](1-\lambda^2\sin^2\alpha)^{-3/2}\} \quad (5)$$

After simplify it's:

$$P_j = \frac{(m_P + m_A) r w^2 [\cos(\alpha+\beta)/\cos\beta + \lambda\cos^2\alpha/\cos^3\beta]}{\cos\beta} \quad (6)$$

Where: m_P is the quality of the piston assembly, m_A is the quality of the small end of the connecting rod, $\lambda = r/l$ is the rod ratio, r is the crank radius, l is the length of the connecting rod, and ω is angular velocity of crankshaft.

$$P_r = m_B r\omega^2 \tag{7}$$

Where: m_B is the quality of the big end of the connecting rod.

The maximum radial force acting on the neck of the crankshaft connecting rod calculated by the above expressions Z_{max} equal 45389.8N.

2.2.4 Load boundary conditions

2.2.4.1 Calculation distribution load of the journal

According to the traditional method and stress distribution of the finite width journal under the oil film pressure, and ignoring the influence of the mutation peak of the pressure at the hole, assume the force boundary conditions are: the law of load distribution along the connecting rod journal and the spindle neck direction is parabolic; the law of load distribution along the circumference direction of the journal is cosine and the regional size is $2\pi/3$ [10-12], as shown in Fig. 3:

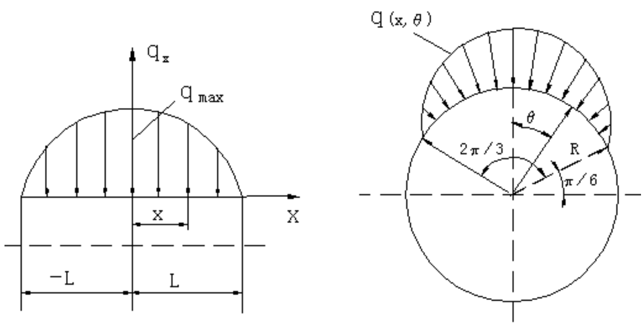

Fig. 3. Force distributions of connecting rod and crankshaft neck.

The following is calculation process of the force boundary:

(1) Along the axis direction of the crankshaft

Assuming the equation of the pressure distribution curve;

$$q_x = ax^2 + bx + c \tag{8}$$

if x=L, -L, q_x =0; if x=0, $q_x = q_{max}$,submit these into the above equation:

$a = -q_{max}/L^2$, b=0, c= q_{max} .

Then get $$q_x = q_{max}(1 - \frac{x^2}{L^2}) \tag{9}$$

(2) Along the circumferential direction of the journal

The law of distribution is Cosine and the equation of the distribution is:

$$q_{(x,\theta)} = q_x \times \cos\kappa\theta \tag{10}$$

if $\theta = \pi/3$, $q_{(x,\theta)} = 0$, that is $\cos\frac{\pi}{3}\kappa = 0$, and the coefficient k= $\frac{\pi}{2}/\frac{\pi}{3}$ =3/2, submit this into equation 10 and get:

$$q_{(x,\theta)} = q_x \times \cos\frac{3}{2}\theta \tag{11}$$

And $Z = \int_{-L}^{L}\int_{-\frac{\pi}{3}}^{\frac{\pi}{3}} q_{(x,\theta)} d_s d_x = 4\int_0^L\int_0^{\frac{\pi}{3}} q_{(x,\theta)} R d_\theta d_x$,

combine equation 9 and equation 11 yield $Z = 4\int_0^L\int_0^{\frac{2}{3}} q_{max}(1-\frac{x^2}{L^2}) \times \cos\frac{3}{2}\theta \times R d_\theta d_x$.

Solve the double integral: $Z = \frac{16}{9} RL \times q_{max}$ that is $q_{max} = \frac{9}{16} \times \frac{Z}{RL}$, the distribution function along the axial and circumferential direction of the pressure is:

$$q_{(x,\theta)} = \frac{9}{16} \times \frac{Z}{RL}(1-\frac{x^2}{L^2}) \times \cos\frac{3}{2}\theta \tag{12}$$

Where: $x = -L \sim \mathrm{L}$, $\theta = -\frac{\pi}{3} \sim \frac{\pi}{3}$, Z is the total load acting on the journal, L is the half-length of crankshaft connecting rod journal, R is radius of the connecting rod journal.

According to the above formula of force distribution, force of each discrete unit can be obtained; in the finite element method, it needs to be transformed into the corresponding concentration force on the node [13]. In order to transform the distribution load of the journal $q_{(x,\theta)}$ into the equivalent nodal force, take any of the rectangle ABCD within the scope of connecting rod journal surface where $q_{(x,\theta)}$ is at work (Fig. 4), the sum of the distribution load in the rectangle ABCD may be calculated by the following two double integrals:

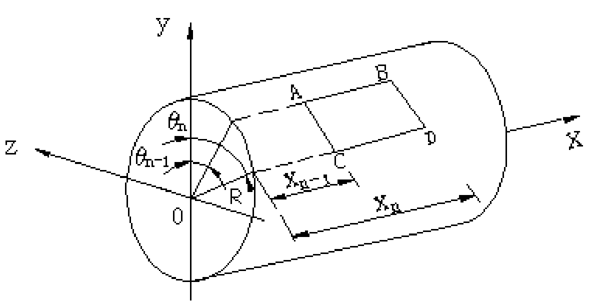

Fig. 4. Calculation of equivalent nodal force.

$$V_z(x,\theta) = -\int_{x_{n-1}}^{x_n}\int_{\theta_{n-1}}^{\theta_n} q_{(x,\theta)} R\sin\theta \times d_x d_\theta \tag{13}$$

$$V_y(x,\theta) = -\int_{x_{n-1}}^{x_n}\int_{\theta_{n-1}}^{\theta_n} q_{(x,\theta)} R\cos\theta \times d_x d_\theta \tag{14}$$

$V_z(x,\theta)$, $V_y(x,\theta)$ is respectively the total load along Z direction and Y direction in the area ABCD, then convert these to the four corners points according to the static equivalence principle. After the equivalent treatment of every element surface under load, superposition the public node force to obtain equivalent nodal boundary forces.

2.2.4.2 The torque transmitted by the flywheel

Transmit the torque acting on the cross-section of the main journal into shear stress changing along the radial direction [14]. Shear stress is fixed along circumference direction, and tangent to the circle, as shown in Fig. 5.

According to the shear stress hypothesis of cross-section torque, it can get:

$$\tau_\rho = \frac{T}{I_p} \times \rho \quad , \quad \text{where}$$

$$I_p = \frac{\pi}{32} \times D^4 \tag{15}$$

Where T is the torque of the flywheel, D is diameter of main journal.

Therefore, transmit the torque into function size force linearly changing with the size of radius.

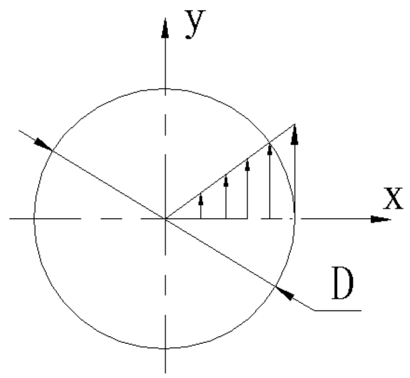

Fig. 5. Distribution of torque shear stress.

3. The analysis of calculation results

3.1 Deformation analysis

When the radial force is the maximum, the axial displacements of the every parts of the crankshaft change in the range of 0.00862 to 0.0112mm. The maximum axial displacement whose value is 0.017mm occurs on the bottom of the right balance block (see Fig. 6). Thus, the deformation of the crankshaft is very small and can meet the design requirements of stiffness of the crankshaft.

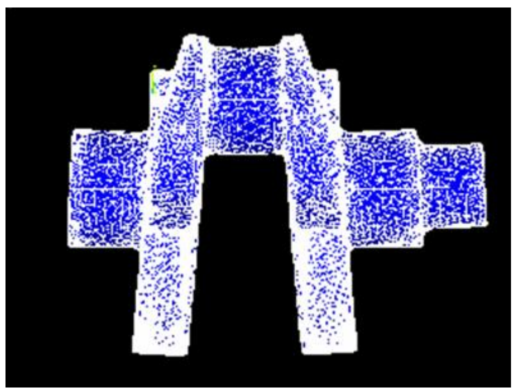

Fig. 6. The deformation cloud of the maximum radial force conditions (enlarged figure).

3.2 Stress analysis

Fig. 7 shows that the larger values of the equivalent stress of the crankshaft arose at the fillet connecting the main journal and the crank, and the lower fillet between the connecting rod journal and the crank, the maximum values occurred at the fillet between the short end of the main journal and the crank arm and its value is 91Mpa. According to the formula for calculating the fatigue factor of safety in the "Engine Design", and the fatigue safety factor of crankshaft n_σ is 4.5. The fatigue safety factor permissible value of crankshaft made of ductile iron $[\ n_\sigma\ ] \geq 1.8$ is usually used. The strength of the crankshaft can meet the requirements.

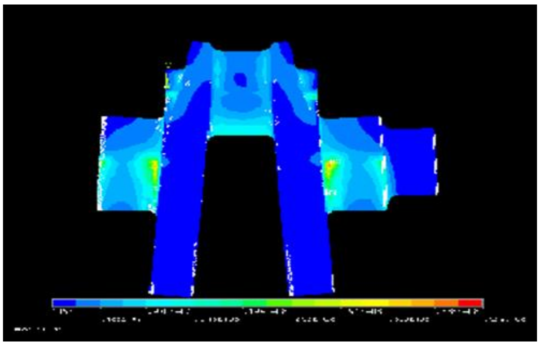

Fig. 7. Principal stress cloud of the maximum radial force condition.

3.3 Modal analysis

After modal calculation using the Lanczos algorithm in ABAQUS, the first 5-order modal frequency was solved as shown in Table 2 and the first and second order mode shape shown in Fig. 8 and Fig. 9.

Table 2. Modal frequency of the crankshaft.

Modal order	1	2	3	4	5	6
Frequence Hz	117.8	151.2	219.1	535	587.1	670.2

From the calculation results, the first and the second modal frequency of the crankshaft avoid the corresponding frequency of the engine operating range (7-22Hz). Working speed of diesel engine is 800 - 2600rpm. According to the natural mode shape obtained from analysis, when crankshaft vibrate in the inherent form of vibration the deformation the spindle neck and connecting rod journal are smaller. The resonance is not likely to happen. Familiar with the bending vibration of crankshaft is very helpful for the analysis of the piston, bearing failure and prevent excessive edge load in the bearing and bearing seat design [15].

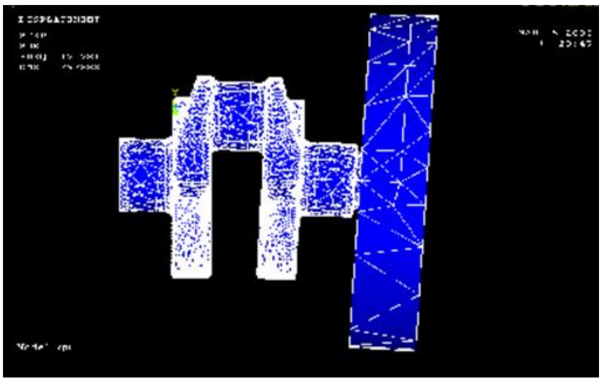

Fig. 8. The first-order vibration shape (f=117.8Hz).

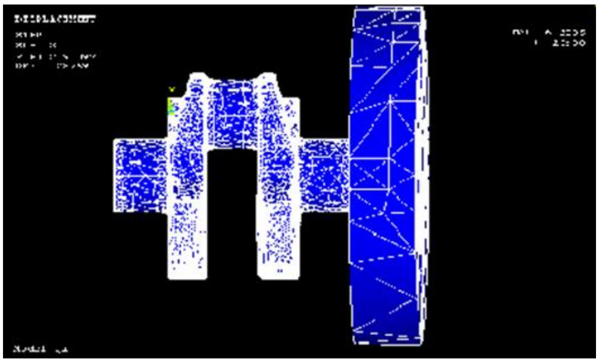

Fig. 9. The second-order vibration shape (f=151.2Hz).

4. Conclusions

(1) The maximum deformation appears at the center of crankpin neck surface. The maximum stress appears at the fillets between the crankshaft journal and crank cheeks, and near the central point of journal. The edge of main journal is high stress area.

(2) The ABAQUS finite element model of the crankshaft is a reasonable model for crankshaft strength, deformation, and modal analysis compared with the traditional simplified method; the simulation results are much closer to the actual situation.

(3) The crankshaft deformation was mainly bending

deformation under the lower frequency. And the maximum deformation was located at the link between main bearing journal and crankpin and crank cheeks. So this area prones to appear the bending fatigue crack. Base on the results, we can forecast the possibility of dynamic interference between the crankshaft and other components. The resonance vibration of system can be avoided effectively by rational structure design. The results provide a valuable theoretical criterion for optimization design of diesel engine.

Acknowledgements

This paper is supported by Creation Project from Shanghai Educational Committee (Project No: 14YZ146), Scientific Start-up Project for Introduction of Talent of Shanghai Institute of Technology (Project No: YJ2011-20), Shanghai Higher Education Connotation Construction 085 Engineering Project (No: 405ZK132124-306) and Shanghai Leading Academic Discipline Project, under J51501.

References

[1] Z. P. Mourelatos, Combustion and engines, **79**, 2009 (2001).
[2] M. Rae, D. Yoon, S. Hyuk, KSME International Journal, **16**, 1095 (2002).
[3] S. T. Han, Z. Y. Hao, Transactions of the Chinese Society of Agricultural Machinery, **32**(4), 74 (2001).
[4] J. Sun, C. L. Gui, X. Li, Transactions of Csice, **20**(2), 179 (2002).
[5] H. Okamura, Proceeding of Vehicle Noise, ASME, **9**(2), 899 (1990).
[6] A. Boysal, H. Rahnejat, Applied Mathematical Modelling, **21**(8), 481 (1997).
[7] Z. M. Fu, D. C. Hu, X. H. Liu, Optoelectron. Adv. Mater. – Rapid Comm. **5**, 1312 (2011).
[8] X. Y. Lei, X. G. Song, D. X. Xue, China Mechanical Engineering, **14**, 1466 (2003).
[9] J. M. Yin, D. H. Wu, Y. H. Yuan, et al., Chinese Internal Combustion Engine Engineering **2**, 71 (1997).
[10] P. Charles, J. K. Sinha, F. Gu, et al., Journal of Sound and Vibration, **321**, 1171 (2009).
[11] H. Okamura, A. Shinno, T. Yamanaka, A. Suzuki, K. Sogabe, ASME, **117**, 71 (1995).
[12] A. A. Smaili, M. P. Khetawat, Mechanism & Machine Theory, **29**, 995 (1994).
[13] P. M. Zissimos, Computers & Structures, **79**, 2009 (2001).
[14] F. Östman, H. T. Toivonen, Control Engineering Practice, **16**, 78 (2008).
[15] X. Zhang, S. D. Yu, Journal of Sound and Vibration, **319**, 491 (2009).

*Corresponding author: wsmsuccess@163.com